

Multimode Diagnosis for Switched Affine Systems with Noisy Measurement

JINGWEI DONG, ARMAN SHARIFI KOLARIJANI AND PEYMAN MOHAJERIN ESFAHANI

ABSTRACT. We study a diagnosis scheme to reliably detect the active mode of discrete-time, switched affine systems in the presence of measurement noise and asynchronous switching. The proposed scheme consists of two parts: (i) the construction of a bank of filters, and (ii) the introduction of a residual/threshold-based diagnosis rule. We develop an exact finite optimization-based framework to numerically solve an optimal bank of filters in which the contribution of the measurement noise to the residual is minimized. The design problem is safely approximated through linear matrix inequalities and thus becomes tractable. We further propose a thresholding policy along with probabilistic false-alarm guarantees to estimate the active system mode in real-time. In comparison with the existing results, the guarantees improve from a polynomial dependency in the probability of false-alarm to a logarithmic form. This improvement is achieved under the additional assumption of sub-Gaussianity, which is expected in many applications. The performance of the proposed diagnosis filters is validated through a synthesis numerical example and an application of the building radiant system.

1. INTRODUCTION

Over the last two decades, special attention has been paid to switched affine systems because they can be used to effectively model a wide range of practical systems, such as chemical plants [1], aeronautic systems [2] and smart buildings [3]. These systems are usually difficult to be exactly described by a single model because of their nonlinear and complex dynamic characteristics. Research on switched systems are mainly focused on identification [4,5], state estimation [6], stability analysis and controller design [7,8]. The prior knowledge of the switching signal that indicates the evolution of modes is crucial for theoretical results in these research topics. For example, a general approach to control switched systems is to employ mode-dependent controllers, where the activation of a proper controller depends on the switching signal. There are, however, several scenarios in which the switching signal is not a priori known. In fault diagnosis scenarios, an unexpected transition from a healthy mode to a faulty mode can be treated as an unknown switching. This implies that one needs to detect the active mode of switched systems. The detection process results in a delay between the active mode and its corresponding controller as well.

1.1. Literature review

The problem of mode detection for switched affine systems has been studied for decades. The proposed approaches can be summarized into two classes: the data-based, and the model-based

The authors are with the Delft Center for Systems and Control, Delft University of Technology, The Netherlands ({J.Dong-6, P.MohajerinEsfahani}@tudelft.nl, Arman.Sh.Kolarigani@gmail.com). This work is partially supported by the ERC grant TRUST-949796 and CSC (China Scholarship Council) with funding number: 201806120015.

approaches. The data-based approaches are most adopted when the parameters of each mode are unknown. In that case, the parameters need to be identified from a collection of input-output data. Then the new data is associated with the most suitable mode through data classification techniques. A number of results on the data-based approaches have been achieved. We refer the interested readers to [4] and the references therein.

Model-based fault diagnosis: In the model-based approaches, one leverages tools from the fault detection and isolation (FDI) field to detect and isolate the changes caused by switching or faults. The most widely used FDI methods are based on residual generation, where certain residual signals are generated by observer-based or parity space methods to quantitatively characterize the occurrence of the changes [9]. Beard [10] proposed the original observer-based diagnosis approach to replace the hardware redundancy in 1971. Many observer-based diagnosis approaches were then developed. To deal with disturbances or noises, the authors in [11] constructed an optimization problem to design the parameters of the observer in which the influence of disturbances on residuals indicated by \mathcal{H}_∞ -norm is minimized. The parity space approach was proposed in [12] which generated residuals to check the consistency between the model and the measurements. It is worthy to note that the constructed residual generators usually have the same order as that of the systems. This makes the generators complex and computationally demanding when dealing with high-dimensional or large-scale systems. Frisk [13] proposed a parity-space-like approach in a polynomial framework which produces residual generators with possibly low order. In their following work [14], the previous approach is extended to the linear differential-algebraic equation (DAE). This extension enlarges the application range of FDI approaches because DAE models cover several classes of models, e.g., transfer functions, state-space models, or descriptor models. The above approaches are for linear systems. For the fault detection of nonlinear systems, a natural way is to linearize the systems at local operating points and decouple the disturbances together with the higher order terms from the residuals, see for example [15, 16]. Another method is to develop adaptive nonlinear estimator to approximate the nonlinear terms [17, 18]. Recently, the authors in [19] developed a tractable optimization-based approach in the DAE framework to design FDI filters to deal with the disturbances and nonlinear terms.

Multi-mode diagnosis: Note that the aforementioned approaches are applicable to systems with a single model. To deal with systems consisting of several modes, a bank of residuals is usually required. Moreover, the systems need to satisfy certain rank conditions to guarantee that any two subsystems can be distinguished from each other. This is called distinguishability (also called discernibility or observability) for switched systems [20, 21]. To detect the active mode, the idea that makes each residual sensitive to all but only one mode is usually adopted, which is called *generalized observer scheme* (GOS) [22]. Following a GOS mindset, results on mode detection are achieved based on basic residual generation methods, such as parity space approaches [23], unknown input observers [24], and sliding mode observers [25]. Another class of mode detection methods is the set-membership method which computes the reachable set of each subsystem. Then, the output is compared to the reachable sets to determine the mode [26, 27]. The authors in [26] developed an active diagnosis approach in which an optimal separating input sequence is designed to guarantee that output sets of different subsystems are separated. In [27], a model invalidation approach was

proposed to compare the input-output data to the nominal behaviors of the system, where the set-membership check was reduced to the feasibility of a mixed integer linear programming problem. The set-membership methods are generally computationally demanding because they require solving optimization problems at each step. Also, the residual generation and set-membership methods mentioned above either neglect the noises or consider noises with deterministic bounds. Hence, they provided guaranteed diagnosis results that are conservativeness.

1.2. Main contributions

In the light of the literature reviewed above, the main message of this paper revolves around a diagnosis scheme to detect the active mode of asynchronously switched affine systems in real-time. The diagnosis scheme consists of a bank of filters and a residual/threshold-based diagnosis rule. The bank of filters comprises as many filters as the admissible mode transition while the diagnosis rule prescribes conditions under which we estimate the transition based on the residual behavior. In particular, the main contributions of this paper are summarized as follows.

- **Exact characterization of an optimal bank of filters:** Building on residual-based detection and \mathcal{H}_2 -norm approaches in the DAE framework, we formulate the optimal bank of filters design problem as a finite optimization problem in which the objective is the noise contribution to the filter residuals (Theorem 3.1). We also provide necessary and sufficient conditions that ensure the feasibility of the resulting optimization problem (Proposition 3.3).
- **Tractable convex restriction:** We provide an LMI-based sufficient condition for the nonlinear constraint in the exact optimization problem of the filters design, leading to a tractable approximation program (Proposition 3.2).
- **Probabilistic performance bounds:** We further propose diagnosis thresholds along with probabilistic false-alarm guarantees to estimate the active system mode (Theorem 3.6). The proposed bound admits a logarithmic dependency with respect to the desired reliability level, which is better than the polynomial rate in the existing works [28]. This improvement comes under the sub-Gaussianity assumption on the noise distribution, a regularity requirement which is expected to hold in many real-world applications.

The rest of the paper is organized as follows. The problem formulation and the proposed architecture of the diagnosis scheme are introduced in Section 2. In Section 3, we present an optimization-based approach to design the filters along with some performance analyses of the proposed scheme. To improve the flow of the paper and its accessibility, we postpone all technical proofs to Section 4. The proposed approach is applied to a numerical example and a building radiant system in Section 5 to validate its effectiveness. Finally, Section 6 concludes the paper with some remarks and future directions.

Notation. Sets $\mathbb{R}_{>0}$ ($\mathbb{R}_{\geq 0}$) and $\mathbb{Z}_{>0}$ ($\mathbb{Z}_{\geq 0}$) denote all positive (non-negative) reals and positive (non-negative) integers, resp. We denote set $\{1, \dots, n\}$ by $[n]$. The sets of symmetric positive semi-definite matrices and non-singular matrices are denoted by \mathcal{S}_+ and \mathcal{N} , resp. We use $*$ to represent the transpose terms in a symmetric matrix. The identity matrix with an appropriate dimension is denoted by I . The maximum singular value of a matrix A is denoted by $\|A\|_2$. For a vector $v = [v_1, \dots, v_n]$, the ℓ_2 and ℓ_∞ norm of v are $\|v\|_2 = \sqrt{\sum_{i \in [n]} v_i^2}$ and $\|v\|_\infty = \max_{i \in [n]} |v_i|$, resp. For

a random variable χ , the probability law and expected value are denoted by $\Pr[\chi]$ and $\mathbf{E}[\chi]$, resp. Given a signal $\{s(k)\}_{k \in \mathbb{Z}_{\geq 0}}$ and an operator \mathbf{O} , the notation $\mathbf{O}[s](k)$ denotes the application of the operator \mathbf{O} on the signal s at the time instance k . The \mathcal{H}_2 -norm of $\mathbf{O}[s]$ is denoted by $\|\mathbf{O}[s]\|_2$.

2. MODEL DESCRIPTION AND PROBLEM STATEMENT

In this section, a formal description of discrete-time asynchronously switched affine systems is given. Then we present the architecture of the proposed diagnosis component and formulate the problems studied in this work.

2.1. Model description

Consider a discrete-time switched affine system that consists of n subsystems:

$$\begin{aligned} x(k+1) &= A_{\sigma(k)}x(k) + B_{\sigma(k)}u(k) + E_{\sigma(k)}d(k), \\ y(k) &= C_{\sigma(k)}x(k) + D_{\sigma(k)}\omega(k) \end{aligned} \quad (1)$$

where $x(k) \in \mathbb{R}^{n_x}$, $u(k) \in \mathbb{R}^{n_u}$ and $y(k) \in \mathbb{R}^{n_y}$ are the state, control input and output, resp. Signal $d(k) \in \mathbb{R}^{n_d}$ represents the constant reference signal, i.e., $d(k) = \bar{d}$. Signal $\omega(k)$ represents the independent identically distributed (i.i.d) measurement noise with zero mean. Map $\sigma(k) : \mathbb{Z}_{>0} \rightarrow [n]$ is a piecewise constant function indicating the active mode. Matrices $A_{\sigma(k)}$, $B_{\sigma(k)}$, $E_{\sigma(k)}$, $C_{\sigma(k)}$ and $D_{\sigma(k)}$ are all known with appropriate dimensions. A constant gain $D_{\sigma(k)}$ is applied to model the level of $\omega(k)$. Without loss of generality, all D_i are set to be equal, i.e., $D_i = D$. For mode $i \in [n]$, the static output-feedback \mathcal{H}_∞ controller u is

$$u(k) = K_i y(k), \quad (2)$$

where K_i is the controller gain. For example, a design method for K_i is proposed in [29]. Let $\mathcal{S} := \{t_s, s \in \mathbb{Z}_{>0}\}$ represents the sequence of switching instances, i.e., $\sigma(t_s) \neq \sigma(t_s - 1)$ for all $t_s \in \mathcal{S}$. Suppose that the switching signal $\sigma(k)$ and switching instance t_s are both unknown to the controller. The controller component keeps instead an estimate $\hat{\sigma}(k)$ of $\sigma(k)$ based on which the controller gain is assigned in the closed-loop dynamics. In the above setting, this work aims to estimate σ through the noisy measurement y in real-time.

2.2. Problem statements

A classical approach to the mode detection problem of switched affine systems is to design a set of individual-mode detectors (or filters), the so-called GOS approach. Under no measurement noise or bounded noise assumption, one is able to provide guaranteed diagnosis results [20, 30]. When there is measurement noise in the dynamics, the residuals could overlap with each other because of the randomness. This brings a challenge to the detection task. In this work, we introduce a diagnosis component as shown in Figure 1 to deal with the problem and challenge. Let \mathbf{S}_{ij} denote the status of the closed-loop dynamics that consists of controller K_i and mode j , then there are in total n^2 closed-loop statuses. For each \mathbf{S}_{ij} , our goal is to design a filter \mathbf{F}_{ij} that generates a meaningful residual $r_{ij} := \mathbf{F}_{ij}[y](k)$ enabling a successful mode detection task. System-theoretically speaking,

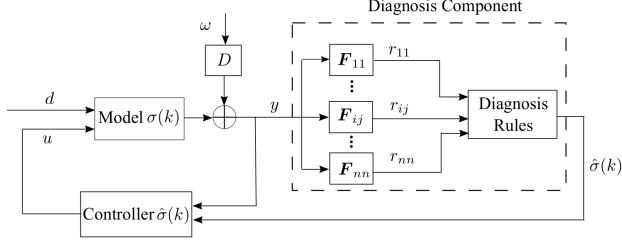


FIGURE 1. Structure of the closed-loop dynamics and diagnosis component

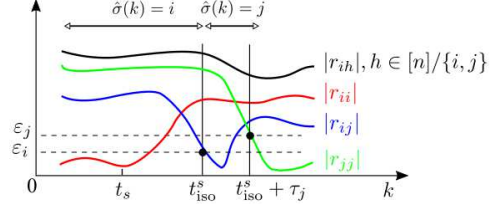


FIGURE 2. Illustration of the diagnosis process

each residual $r_{ij}(k)$ is a function of signals $d(k)$ and $\omega(k)$. So, we enforce the following input-output maps

$$d \xrightarrow{S_{ij}} r_{ij} = 0, \quad (3a)$$

$$d \xrightarrow{S_{ih}} r_{ij} \neq 0, \quad \forall h \in [n]/\{j\}, \quad (3b)$$

$$\omega \xrightarrow{S_{ih}} r_{ij} \leq \eta_{ij}^{S_{ih}}, \quad \forall h \in [n], \quad (3c)$$

through each filter F_{ij} . In particular, condition (3a) tries to decouple d from r_{ij} when the status is S_{ij} . Condition (3b) guarantees that the contribution of d to r_{ij} is nonzero when the status is S_{ih} for $h \in [n]/\{j\}$. Condition (3c) is introduced to suppress the impact of the noise on r_{ij} for all statuses, where $\eta_{ij}^{S_{ih}} \in \mathbb{R}_{\geq 0}$ denotes the gain from ω to r_{ij} . To isolate the correct mode, we only compare the residuals that share the same index representing the controller, i.e., $r_{\hat{\sigma}j}$ for $j \in [n]$, because $\hat{\sigma}(k)$ is always known. The first problem addressed in this paper is the design of the filters, which is stated as follows.

Problem 1. (Optimal bank of filters) Consider the closed-loop dynamics (1)-(2) and the architecture of the diagnosis component in Figure 1. Design the filters F_{ij} for all $i, j \in [n]$, such that the mapping relationships (3) are satisfied and the effect of ω on r_{ij} is suppressed for all S_{ih} where $h \in [n]$, i.e.,

$$\min_{F_{ij}} \left\{ \sum_{h=1}^n \eta_{ij}^{S_{ih}} : (3a), (3b), (3c) \right\}. \quad (4)$$

Given the filters, we now shift attention to the diagnosis rule. Figure 2 illustrates the mechanism of the rule. Let $\varepsilon_i \in \mathbb{R}_{>0}$ and $\tau_i \in \mathbb{Z}_{>0}$ be two user-defined scalars for each mode $i \in [n]$, where ε_i denotes the residual threshold and τ_i denotes a period of time (called the *waiting time*). A transition from mode i to mode j at t_s is denoted by $M_{i \rightarrow j}^{t_s}$. The time when $M_{i \rightarrow j}^{t_s}$ is isolated is denoted by t_{iso}^s . Suppose that S_{ii} is the closed-loop status before t_s . One can see from Figure 2 that $|r_{ii}(k)| \leq \varepsilon_i$ and $|r_{ih}(k)| > \varepsilon_i$ for all $h \neq i$ before t_s , thus $\hat{\sigma}(k) = i$. After $M_{i \rightarrow j}^{t_s}$ happens, the estimated signal $\hat{\sigma}(k)$ cannot be determined immediately and thus remains unchanged. The new mode j is isolated and the corresponding controller K_j is activated when there is only $|r_{ij}(k)|$ being smaller than ε_i at t_{iso}^s . Then, the controller is set to $\hat{\sigma}(k) = j$ and wait for a period of time τ_j to let $|r_{jj}(k)|$ reach the threshold ε_j . As a result, the diagnosis rules to determine $\hat{\sigma}(k+1)$ based on the residuals $r_{\hat{\sigma}j}(k)$,

waiting time $\tau_{\hat{\sigma}(k)}$, and $\hat{\sigma}(k)$ are described through

$$j^*(k) = \arg \min_{j \in [n]} |r_{\hat{\sigma}j}(k)|, \quad (5a)$$

$$t_{\text{iso}}(k) = \max \{t \in \mathbb{Z}_{>0} : \hat{\sigma}(t) \neq \hat{\sigma}(t-1), k \geq t\}, \quad (5b)$$

$$\hat{\sigma}(k+1) = \begin{cases} j^*(k), & \begin{cases} |r_{\hat{\sigma}j^*}(k)| \leq \varepsilon_{\hat{\sigma}(k)} < \min_{j \neq j^*(k)} |r_{\hat{\sigma}j}(k)| \\ \text{and } k \geq t_{\text{iso}}(k) + \tau_{\hat{\sigma}(k)} \end{cases} \\ \hat{\sigma}(k), & \text{otherwise.} \end{cases} \quad (5c)$$

Let us briefly highlight the meaning of each relation of the diagnosis rule (5): In (5a), the index $j^*(k)$ represents the system mode whose corresponding residual $r_{\hat{\sigma}j}(k)$ has the minimum absolute value across all $j \in [n]$. In (5b), the time $t_{\text{iso}}(k)$ denotes the last switching instance of $\hat{\sigma}$, and finally (5c) updates the estimation of the system mode at the next time instant. In the case of incorrect isolation, according to (5), the diagnosis component will wait for some time, and then compare the residuals $r_{\hat{\sigma}j}$ for $j \in [n]$ to isolate the correct mode again.

Note that the threshold ε_i and waiting time τ_j are parameters to be determined. The main objective of these two parameters is to detect the current mode of the system, say $\sigma(k) = j$. Knowing the current controller mode $\hat{\sigma}(k) = i$, this goal is closely related to the behavior of the matched filter residual r_{ij} . It is worth pointing out that the incorrect isolation (i.e., $\hat{\sigma}(t_{\text{iso}}^s) \neq \sigma(t_{\text{iso}}^s)$) is inevitable due to the stochastic nature of the system measurements. The second problem studied in this work is aiming to formalize this requirement as the basis to adjust the threshold ε_i and the waiting time τ_j for all $i, j \in [n]$.

Problem 2. (Probabilistic performance certificates) Suppose that transition $M_{i \rightarrow j}^{t_s}$ occurs (i.e., $\sigma(t_s) = j, \hat{\sigma}(t_s) = i$). Given the designed filters from Problem 1 and a reliability level $\beta \in (0, 1]$, determine the threshold ε_i and the estimated matched time T_{ij} such that

$$\Pr[|r_{ij}(k)| \leq \varepsilon_i \mid M_{i \rightarrow j}^{t_s}] \geq 1 - \beta, \quad \forall t_s + T_{ij} \leq k \leq t_{s+1}. \quad (6)$$

Remark 2.1. (Waiting time) The waiting time τ_j depicted in Figure 2 is indeed a special case of the estimated matched time introduced in Problem 2 where the controller and system modes coincide, i.e., $\hat{\sigma}(t_{\text{iso}}^s) = \sigma(t_{\text{iso}}^s) = j$, and as such $\tau_j = T_{jj}$.

If the next transition occurs before $t_s + T_{ij}$, the guarantee in (6) is no longer useful. In fact, the transition frequency is an inherent difficulty of mode detection in this context. People refer to the time between two consecutive transitions as *dwell time* [8]. We introduce the following assumption to guarantee that the system stays in one mode long enough. Generally, the dwell time of a real system is much longer than the time used to detect the mode. Thus, it is justifiable to make such an assumption.

Assumption 2.2. (Dwell time) For all $t_s \in \mathcal{S}$, there exists a large enough positive constant τ_d which satisfies $t_{s+1} - t_s \geq \tau_d$, so that Problem 2 is feasible.

3. MAIN RESULT

In this section, we present the expression and design method of the diagnosis filters first. Then, the computation methods of the thresholds and estimated matched time are given to provide probabilistic guarantees on the diagnosis performance. All proofs are moved to section 4 to improve the readability.

3.1. Filter design: optimization-based method

Considering the asynchronous switching, we first write the closed-loop dynamics (1)-(2) into

$$\begin{aligned} x(k+1) &= A_{ij}^{cl}x(k) + E_j d(k) + B_j K_i D \omega(k) \\ y(k) &= C_j x(k) + D \omega(k), \end{aligned} \quad (7)$$

where $A_{ij}^{cl} = A_j + B_j K_i C_j$. In order to present the expression of the filters, we further reformulate (7) into the DAE format, which is

$$H_{ij}(\mathbf{q})X(k) + L(\mathbf{q})y(k) + G_{ij}(\mathbf{q})\omega(k) = 0 \quad (8)$$

where $X(k) = [x(k)^\top \ d(k)^\top]^\top$. The operator \mathbf{q} is a time-shift operator, i.e., $X(k+1) = \mathbf{q}X(k)$. The polynomial matrices $H_{ij}(\mathbf{q})$, $L(\mathbf{q})$ and $G_{ij}(\mathbf{q})$ are

$$H_{ij}(\mathbf{q}) = H_{ij,1}\mathbf{q} + H_{ij,0} = \begin{bmatrix} -\mathbf{q}I + A_{ij}^{cl} & E_j \\ C_j & 0 \end{bmatrix}, \quad L(\mathbf{q}) = L_0 = \begin{bmatrix} 0 \\ -I \end{bmatrix}, \quad G_{ij}(\mathbf{q}) = G_{ij,0} = \begin{bmatrix} B_j K_i D \\ D \end{bmatrix}.$$

Inspired by [14] and [19], the filter \mathbf{F}_{ij} is defined as

$$\mathbf{F}_{ij}(\mathbf{q}) = a^{-1}(\mathbf{q})N_{ij}(\mathbf{q})L(\mathbf{q}), \quad (9)$$

where the polynomial row vector $N_{ij}(\mathbf{q}) = \sum_{m=0}^{d_N} N_{ij,m}\mathbf{q}^m$, $N_{ij,m} \in \mathbb{R}^{1 \times (n_x + n_y)}$ are constant row vectors, d_N denotes the degree of $N_{ij}(\mathbf{q})$, and $a(\mathbf{q})$ is a $(d_N + 1)$ -th order polynomial with all roots inside the unit disk. Both $N_{ij}(\mathbf{q})$ and $a(\mathbf{q})$ are the design parameters in (9). To simplify the design process, we fix $a(\mathbf{q})$ here, and find a feasible $N_{ij}(\mathbf{q})$. We define

$$a(\mathbf{q}) = \mathbf{q}^{d_N+1} + a_{d_N}\mathbf{q}^{d_N} + \cdots + a_1\mathbf{q} + a_0, \quad (10)$$

where a_m is a constant coefficient for each $m \in \{0, 1, \dots, d_N\}$. Notice that the role of $a(\mathbf{q})$ is to ensure that the obtained filter \mathbf{F}_{ij} is proper and stable. For the sake of simplicity of exposition, we suppose that all the filters are of the same degree. With the DAE model (8) and the definition of filter \mathbf{F}_{ij} in (9), the mapping relationships from d and ω to r_{ij} are obtained through multiplying from left of (8) by $a^{-1}(\mathbf{q})N_{ij}(\mathbf{q})$, that is

$$r_{ij}(k) = \frac{N_{ij}(\mathbf{q})L(\mathbf{q})}{a(\mathbf{q})}y(k) = -\frac{N_{ij}(\mathbf{q})H_{ij}(\mathbf{q})}{a(\mathbf{q})}X(k) - \frac{N_{ij}(\mathbf{q})G_{ij}(\mathbf{q})}{a(\mathbf{q})}\omega(k). \quad (11)$$

To employ tools in robust control to deal with the noise, we derive the observable canonical form of \mathbf{F}_{ij} based on (9), which is

$$\begin{aligned} \bar{x}_{ij}(k+1) &= A_r \bar{x}_{ij}(k) + B_{r_{ij}} y(k) \\ r_{ij}(k) &= C_r \bar{x}_{ij}(k), \end{aligned} \quad (12)$$

where $\tilde{x}_{ij}(k) \in \mathbb{R}^{d_N+1}$ denotes the state. Matrices $A_r, B_{r_{ij}}, C_r$ are given by

$$A_r = \begin{bmatrix} 0 & \dots & 0 & -a_0 \\ 1 & \dots & 0 & -a_1 \\ \vdots & \ddots & \vdots & \vdots \\ 0 & \dots & 1 & -a_{d_N} \end{bmatrix}, \quad B_{r_{ij}} = \begin{bmatrix} N_{ij,0} \\ N_{ij,1} \\ \vdots \\ N_{ij,d_N} \end{bmatrix} L_0, \quad C_r = [0 \dots 0 \ 1]. \quad (13)$$

Note that the coefficients of the design parameter $N_{ij}(\mathbf{q})$ are reformulated into $B_{r_{ij}}$. Furthermore, to deal with the unmatched residuals, we introduce the augmented state $\tilde{x}_{ij} = [x(k)^\top \ \tilde{x}_{ij}(k)^\top]^\top$. When the status is S_{ih} , the dynamics of \tilde{x}_{ij} can be derived from (7) and (12), which is

$$\begin{aligned} \tilde{x}_{ij}(k+1) &= \tilde{A}_{ij}^{S_{ih}} \tilde{x}_{ij}(k) + \tilde{E}_h d(k) + \tilde{D}_{ij}^{S_{ih}} \omega(k) \\ r_{ij}(k) &= \tilde{C}_r \tilde{x}_{ij}(k), \end{aligned} \quad (14)$$

where

$$\tilde{A}_{ij}^{S_{ih}} = \begin{bmatrix} A_{ih}^{cl} & 0 \\ B_{r_{ij}} C_h & A_r \end{bmatrix}, \quad \tilde{E}_h = \begin{bmatrix} E_h \\ 0 \end{bmatrix}, \quad \tilde{D}_{ij}^{S_{ih}} = \begin{bmatrix} B_h K_i D \\ B_{r_{ij}} D \end{bmatrix}, \quad \tilde{C}_r = [0 \ C_r].$$

Here, the design parameter $B_{r_{ij}}$ is contained in $\tilde{A}_{ij}^{S_{ih}}$ and $\tilde{D}_{ij}^{S_{ih}}$.

Before presenting the design method of the filters parameters, let us introduce several notations. Let $\mathbf{T}_{dr_{ij}}^{S_{ih}}(\mathbf{q})$ and $\mathbf{T}_{\omega r_{ij}}^{S_{ih}}(\mathbf{q})$ denote the transfer functions from d and ω to r_{ij} when the status is S_{ih} , resp. The upper bound of \mathcal{H}_2 -norm of $\mathbf{T}_{\omega r_{ij}}^{S_{ih}}(\mathbf{q})$ is denoted by $\sqrt{\eta_{ij}^{S_{ih}}}$, i.e., $\|\mathbf{T}_{\omega r_{ij}}^{S_{ih}}(\mathbf{q})\|_2^2 \leq \eta_{ij}^{S_{ih}}$. To design filters satisfying conditions in Problem 1, we formulate an optimization problem in the following Theorem.

Theorem 3.1 (Optimal bank of filters: exact finite reformulation). *Consider the closed-loop dynamics (1)-(2) and the filter \mathbf{F}_{ij} proposed in (9) with the state-space realization $(A_r, B_{r_{ij}}, C_r)$ as defined in (13). Let us interpret the mapping requirement in (3b) as the steady-state gain. Then, Problem 1 as defined in (4) can be equivalently translated into the following finite optimization program:*

$$\begin{aligned} \min \quad & \sum_{m=1}^n \eta_{ij}^{S_{im}} \\ \text{s.t.} \quad & \forall m \in [n], \forall h \in [n]/\{j\}, \eta_{ij}^{S_{im}} \in \mathbb{R}_{\geq 0}, Z_{ij}^{S_{im}} \in \mathbb{R}_{\geq 0}, P_{ij}^{S_{ij}} \in \mathcal{S}_+^{d_N+1}, P_{ij}^{S_{ih}} \in \mathcal{S}_+^{n_x+d_N+1}, \\ & \bar{N}_{ij} \bar{H}_{ij} = 0, \end{aligned} \quad (15a)$$

$$\|a^{-1}(1) \bar{N}_{ij} \mathcal{L}_{ih}\|_\infty \geq 1 \quad (15b)$$

$$\begin{bmatrix} P_{ij}^{S_{ij}} & A_r P_{ij}^{S_{ij}} & B_{\omega r_{ij}}^{S_{ij}} \\ * & P_{ij}^{S_{ij}} & 0 \\ * & * & I \end{bmatrix} \succeq 0, \quad \begin{bmatrix} Z_{ij}^{S_{ij}} & C_r P_{ij}^{S_{ij}} \\ * & P_{ij}^{S_{ij}} \end{bmatrix} \succeq 0, \quad Z_{ij}^{S_{ij}} \leq \eta_{ij}^{S_{ij}}, \quad (15c)$$

$$\begin{bmatrix} P_{ij}^{S_{ih}} & \tilde{A}_{ij}^{S_{ih}} P_{ij}^{S_{ih}} & \tilde{D}_{ij}^{S_{ih}} \\ * & P_{ij}^{S_{ih}} & 0 \\ * & * & I \end{bmatrix} \succeq 0, \quad \begin{bmatrix} Z_{ij}^{S_{ih}} & \tilde{C}_r P_{ij}^{S_{ih}} \\ * & P_{ij}^{S_{ih}} \end{bmatrix} \succeq 0, \quad Z_{ij}^{S_{ih}} \leq \eta_{ij}^{S_{ih}}, \quad (15d)$$

where the involved matrices are given by

$$\bar{N}_{ij} = [N_{ij,0} \ N_{ij,1} \ \dots \ N_{ij,d_N}], \quad \mathcal{L}_{ih} = \bar{L} \overbrace{[I \ \dots \ I]}^{d_N+1} C_h (I - A_{ih}^{cl})^{-1} E_h,$$

$$\bar{H}_{ij} = \begin{bmatrix} H_{ij,0} & H_{ij,1} & \dots & 0 \\ \vdots & \ddots & \ddots & \vdots \\ 0 & \dots & H_{ij,0} & H_{ij,1} \end{bmatrix}, B_{\omega r_{ij}}^{S_{ij}} = - \begin{bmatrix} N_{ij,0} \\ \vdots \\ N_{ij,d_N} \end{bmatrix} G_{ij,0}, \bar{L} = \begin{bmatrix} L_0, & \dots, & 0 \\ \vdots & \ddots & \vdots \\ 0 & \dots & L_0 \end{bmatrix}.$$

Proof. The proof is provided in Section 4.1. \square

Observe that (15) is not a convex optimization problem because (15b) and (15d) are non-convex constraints. However, (15b) can be reformulated into a union of several linear constraints, i.e.,

$$a^{-1}(1)\bar{N}_{ij}\mathcal{L}_{ih}e_l \geq 1, \text{ or } a^{-1}(1)\bar{N}_{ij}\mathcal{L}_{ih}e_l \leq -1,$$

where $e_l = [0 \dots 1 \dots 0]^\top$ for $l \in [n_d]$. To deal with the nonlinear term $\tilde{A}_{ij}^{S_{ih}} P_{ij}^{S_{ih}}$ in (15d), one can use Alternating Optimization (AO) method. The decision variables in (15) are divided into two sets, i.e., $\{\bar{N}_{ij}, P_{ij}^{S_{ij}}, \eta_{ij}^{S_{im}}, Z_{ij}^{S_{im}} : m \in [n]\}$ and $\{P_{ij}^{S_{ih}} : h \in [n]/\{j\}\}$. Then, AO solves (15) by alternating minimization over the two sets of variables iteratively.

The following Proposition shows that the nonlinear matrix inequality in (15d) can also be safely approximated with an LMI.

Proposition 3.2 (Optimal bank of filters: safe convex approximations). *Consider the optimization problem (15). The nonlinear inequality constraint as the first term in (15d) can be safely approximated for constants $\alpha \in \mathbb{R}$ and $\gamma \in \mathbb{R}_{>0}$ via the following LMI constraint:*

$$\begin{bmatrix} P_{ij}^{S_{ih}} & \hat{A}_{ih} G_{ij}^{S_{ih}} & \hat{B}_{r_{ij}} & 0 \\ * & \Xi_{ij}^{S_{ih}} & 0 & (\hat{D}_h G_{ij}^{S_{ih}})^\top \\ * & * & \frac{1}{\gamma} I & 0 \\ * & * & * & \gamma I \end{bmatrix} \succeq 0, \quad (16)$$

where the involved matrices are defined as

$$\hat{A}_{ih} = \begin{bmatrix} \begin{bmatrix} A_{ih}^{cl} & 0 \\ 0 & A_r \end{bmatrix} & \begin{bmatrix} B_h K_i D \\ 0 \end{bmatrix} \end{bmatrix}, G_{ij}^{S_{ih}} = \begin{bmatrix} G_{ij,1}^{S_{ih}} & 0 \\ 0 & G_{ij,2}^{S_{ih}} \end{bmatrix}, G_{ij,1}^{S_{ih}} \in \mathcal{N}^{n_x+d_N+1}, G_{ij,2}^{S_{ih}} \in \mathcal{N}^{n_\omega},$$

$$\hat{D}_h = \begin{bmatrix} \begin{bmatrix} C_h & 0 \end{bmatrix} & D \end{bmatrix}, \hat{B}_{r_{ij}} = \begin{bmatrix} 0 \\ -B_{r_{ij}} \end{bmatrix}, \Xi_{ij}^{S_{ih}} = \alpha G_{ij}^{S_{ih}} + \alpha G_{ij}^{S_{ih}\top} - \alpha^2 \begin{bmatrix} P_{ij}^{S_{ih}} & 0 \\ * & I \end{bmatrix}.$$

Proof. The proof is provided in Section 4.1. \square

Furthermore, we provide necessary and sufficient conditions for the feasibility of the optimization problem (15) in the following Proposition. Here, the rank and eigenvalues of a matrix A are denoted by $\text{Rank}(A)$ and $\Lambda(A)$, resp.

Proposition 3.3 (Optimal bank of filters: feasibility). *The optimization problem (15) is feasible if and only if the following conditions are satisfied.*

$$(d_N + 1)(n_x + n_y) > \text{Rank}(\bar{H}_{ij}), \quad (17a)$$

$$\text{Rank}([\bar{H}_{ij} \ \mathcal{L}_{ih}]) > \text{Rank}(\bar{H}_{ij}), \quad (17b)$$

$$|\Lambda(A_r)| < 1, |\Lambda(A_{ih}^{cl})| < 1, \text{ (i.e., } A_r \text{ and } A_{ih}^{cl} \text{ are stable)}. \quad (17c)$$

Proof. The proof is provided in Section 4.1. □

Note that the solutions to (15) are not unique because they depend on the degree d_N . This makes it possible to construct filters with lower order compared to that of the systems. The inequality (17a) provides a way to find the minimum d_N . According to (17c), $|\Lambda(A_{ih}^{cl})| < 1$ ensures that (15d) is feasible. However, A_{ih}^{cl} could be unstable because the model and controller are unmatched. Hence, the constraints in (15d) with unstable A_{ih}^{cl} should be excluded. Since the unmatched residuals of those unstable modes diverge from zero, removing those constraints has no effect on the mode detection task.

3.2. Performance certificates

With the designed filters, we now determine the threshold ε_i and waiting time τ_j to ensure proper detection task governed by (5). Considering the stochastic measurement noise ω , we resort to the probabilistic guarantees depicted in (6). Let us first introduce the following lemma and assumption.

Lemma 3.4 (Sub-Gaussian concentration [31, Proposition 2.5.2]). *Suppose χ is an \mathbb{R}^{n_x} -valued sub-Gaussian random vector with positive parameter C_χ , i.e., $\mathbf{E}[e^{\phi\nu^\top(\chi - \mathbf{E}[\chi])}] \leq e^{C_\chi^2\phi^2/2}$ for all $\phi \in \mathbb{R}$ and $\nu \in \mathbb{R}^{n_x}$ where $\|\nu\|_2 = 1$. Then, we have*

$$\Pr[\|\chi - \mathbf{E}[\chi]\|_\infty \leq \varepsilon] \geq 1 - 2n_\chi e^{-\frac{\varepsilon^2}{2C_\chi^2}}, \quad \forall \varepsilon \in \mathbb{R}_{>0}. \quad (18)$$

Assumption 3.5 (Sub-Gaussian noise). *The measurement noise ω is i.i.d. sub-Gaussian signal as defined in Lemma 3.4, with zero mean and parameter $C_\omega \in \mathbb{R}_{>0}$.*

From (18), the tails of sub-Gaussian distributions decay exponentially. Moreover, the class of sub-Gaussian distributions is wide which contains Gaussian, Bernoulli, and all bounded distributions. Thus, we assume the noise to be sub-Gaussian in this work. In order to improve the readability, let us further introduce several notations before presenting the results. Let the polynomial row vector $N_{ij}(\mathbf{q}) := [\hat{N}_{ij}(\mathbf{q}) \check{N}_{ij}(\mathbf{q})]$, where $\hat{N}_{ij}(\mathbf{q})$ and $\check{N}_{ij}(\mathbf{q})$ have dimensions n_x and n_y , resp. Define $\lambda_{\max} := \max_{m \in [d_N+1]} |\lambda_m|$, where λ_m is a root of $a(\mathbf{q})$ defined in (10). These roots are chosen to be distinct, i.e., $\lambda_m \neq \lambda_n$ for $m \neq n$. The following Theorem provides conditions for the probabilistic performance certificates.

Theorem 3.6 (Probabilistic performance certificates). *Suppose Assumption 3.5 holds and consider the closed-loop dynamics (1)-(2), the designed filter \mathbf{F}_{ij} , and the corresponding optimal solutions $\eta_{ij}^{S_{ij}^*}$ from (15). Given the reliability $\beta \in (0, 1]$ and a constant $\mu \in \mathbb{R}_{>0}$, the probabilistic performance (6) in Problem 2 is satisfied, if the threshold ε_i is set as*

$$\varepsilon_i = (\mu + \sqrt{2 \ln(2/\beta)}) \sqrt{\bar{\eta}_i} \text{ where } \bar{\eta}_i = \max_{j \in [n]} \eta_{ij}^{S_{ij}^*}, \quad (19)$$

and the estimated matched time T_{ij} equals to

$$T_{ij} = \left\lceil \log_{\lambda_{\max}} \frac{\mu \sqrt{\bar{\eta}_i}}{\psi_{ij}(\mathbf{F}_{ij}, \tilde{x}_{ij}(t_s))} \right\rceil, \quad (20)$$

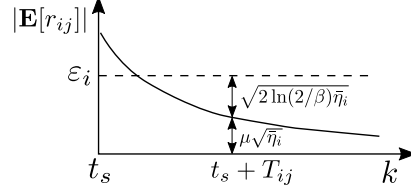


FIGURE 3. Estimated matched time

where $\psi_{ij}(\mathbf{F}_{ij}, \tilde{x}_{ij}(t_s)) = \sqrt{d_N + 1}(1 + \lambda_{\max}^{-1} \|\bar{B}_{r_{ij}}\|_2) \|\mathbf{E}[\tilde{x}_{ij}(t_s)]\|_2$. The matrix $\bar{B}_{r_{ij}}$ is defined as

$$\bar{B}_{r_{ij}} = \begin{bmatrix} b_{ij,11} & \cdots & b_{ij,1n_x} \\ \vdots & \ddots & \vdots \\ b_{ij,(d_N+1)1} & \cdots & b_{ij,(d_N+1)n_x} \end{bmatrix},$$

where $b_{ij,lh} = -\frac{\sum_{m=0}^{d_N} \hat{N}_{ij,m}(h) \lambda_l^m}{\prod_{\tilde{l} \neq l} (\lambda_{\tilde{l}} - \lambda_l)}$ for $h \in [n_x]$, $l, \tilde{l} \in [d_N + 1]$, and $\hat{N}_{ij,m}(h)$ denotes the h -th element of $\hat{N}_{ij,m}$.

Proof. The proof is provided in Section 4.2. \square

The estimated matched time T_{ij} in (20) is actually an upper bound for the time that $\|\mathbf{E}[r_{ij}]\|_2$ takes to arrive at $\mu\sqrt{\eta_i}$ after transition happens (as shown in Figure 3). Then, we set the confidence interval according to β , such that ε_i is determined.

Remark 3.7 (Trade-off analysis). *There is a trade off in selecting μ and β in (19). In particular, a smaller threshold provides high guarantees on excluding the unmatched residuals. We can decrease the threshold with smaller μ or larger β . However, a smaller μ leads to a more conservative estimated matched time. Also, a larger β increases the chance of false detection.*

Remark 3.8 (Comparison with Chebyshev based bounds). *We highlight that the threshold (19) depends logarithmically on the reliability parameter, i.e., $\sqrt{\ln(2/\beta)}$. This is a significant improvement in comparison with the results based on Chebyshev's inequality (e.g., [28, Section III.B]) in which the threshold scales polynomially by the factor $\sqrt{1/\beta}$.*

As a special case of T_{ij} in Theorem 3.6, the waiting time τ_j can be determined by

$$\tau_j = \left\lceil \log_{\lambda_{\max}} \frac{\mu\sqrt{\eta_j}}{\psi_{jj}(\mathbf{F}_{jj}, \tilde{x}_{jj}(t_{\text{iso}}^s))} \right\rceil, \quad (21)$$

where $\psi_{jj}(\mathbf{F}_{jj}, \tilde{x}_{jj}(t_{\text{iso}}^s)) = \sqrt{d_N + 1}(1 + \lambda_{\max}^{-1} \|\bar{B}_{r_{jj}}\|_2) \|\mathbf{E}[\tilde{x}_{jj}(t_{\text{iso}}^s)]\|_2$. Observe that the expected values $\tilde{x}_{ij}(t_s)$ and $\tilde{x}_{jj}(t_{\text{iso}}^s)$ still need to be computed in (20) and (21). Thanks to Assumption 2.2, we assume that the system is in the steady state at t_s . Then, $\mathbf{E}[\tilde{x}_{ij}(t_s)]$ can be obtained by $\mathbf{E}[\tilde{x}_{ij}(t_s)] = (I - \tilde{A}_{ij}^{S_{ii}})^{-1} \tilde{E}_i \bar{d}$. For $\mathbf{E}[\tilde{x}_{jj}(t_{\text{iso}}^s)]$, we first compute $\mathbf{E}[\tilde{x}_{jj}(t_s + T_{ij})]$ because the diagnosis time is an unknown random value. According to the closed-loop dynamics (14), we have

$$\mathbf{E}[\tilde{x}_{jj}(t_s + T_{ij})] = \tilde{A}_{jj}^{S_{ij} T_{ij}} \mathbf{E}[\tilde{x}_{jj}(t_s)] + \sum_{m=0}^{T_{ij}-1} \tilde{A}_{jj}^{S_{ij} T_{ij} - 1 - m} \tilde{E}_j \bar{d},$$

where $\mathbf{E}[\tilde{x}_{jj}(t_s)]$ is also computed in the steady state. Then, taking all transitions to mode j into account, we compute the value $\max_{i \in [n]} \|\mathbf{E}[\tilde{x}_{jj}(t_s + T_{ij})]\|_2$ as an alternative of $\|\mathbf{E}[\tilde{x}_{jj}(t_{\text{iso}}^s)]\|_2$.

According to the diagnosis rule (5), one still needs to let the unmatched residuals be outside the threshold interval. Suppose the status is S_{ij} . Inspired by the active fault diagnosis method [26], we design the reference signal d such that the unmatched residuals r_{ih} satisfy $|\mathbf{E}[r_{ih}]| \geq \varepsilon_i + \bar{\mu}\sqrt{\bar{\eta}_i}$ where $\bar{\mu} \in \mathbb{R}_{>0}$ is a constant. From the closed-loop dynamics (7) and (11), the unmatched residual $r_{ih}(k)$ can be written as

$$\begin{aligned} r_{ih}(k) &= \frac{N_{ih}(\mathbf{q})L(\mathbf{q})}{a(\mathbf{q})} \left[C_j(\mathbf{q}I - A_{ij}^{cl})^{-1} (E_j d(k) + B_j K_i D \omega(k)) + D \omega(k) \right] \\ &= \mathbf{T}_{dr_{ih}}^{S_{ij}}(\mathbf{q})[d](k) + \mathbf{T}_{\omega r_{ih}}^{S_{ij}}(\mathbf{q})[\omega](k), \end{aligned} \quad (22)$$

According to (22), the expected value $\mathbf{E}[r_{ih}] = a^{-1}(1)\bar{N}_{ih}\mathcal{L}_{ij}\bar{d}$. As a result, the requirement $|\mathbf{E}[r_{ih}]| \geq \varepsilon_i + \bar{\mu}\sqrt{\bar{\eta}_i}$ is equivalent to choosing \bar{d} such that

$$|a^{-1}(1)\bar{N}_{ih}\mathcal{L}_{ij}\bar{d}| \geq \varepsilon_i + \bar{\mu}\sqrt{\bar{\eta}_i}. \quad (23)$$

In light of Lemma 3.4, r_{ih} will be larger than or equal to ε_i with guaranteed probability in the steady state if (23) is satisfied.

Remark 3.9 (Regularities on the reference input). *When design the filters and thresholds, the value of the reference signal is not necessary. However, the value of the reference signal is required when computing the estimated matched time T_{ij} . Moreover, in order to separate the residuals of different modes in the presence of noise, the reference signal \bar{d} should satisfy (23). Such constraint is not novel in the distinguishability problem for switched affine systems [32]. This also can be interpreted as the persistence of excitation.*

4. TECHNIQUE PROOFS OF MAIN RESULTS

This section presents the technical proofs of the theoretical results in Section 3.

4.1. Proofs of results in filter design

Let us start with two lemmas required for the proof of Theorem 3.1.

Lemma 4.1. *(Multiplication of polynomial matrices [19, Section III-A]) Let $Q_1(\mathbf{q})$ and $Q_2(\mathbf{q})$ be polynomial matrices of degree d_1 and d_2 , resp, and defined by*

$$Q_1(\mathbf{q}) = \sum_{m=0}^{d_1} Q_{1,m} \mathbf{q}^m, \quad Q_2(\mathbf{q}) = \sum_{m=0}^{d_2} Q_{2,m} \mathbf{q}^m,$$

where $Q_{1,m} \in \mathbb{R}^{n_1 \times n_2}$ and $Q_{2,m} \in \mathbb{R}^{n_2 \times n_3}$ are the matrices of constant coefficients. The multiplication of $Q_1(\mathbf{q})$ and $Q_2(\mathbf{q})$ is equivalent to

$$Q_1(\mathbf{q})Q_2(\mathbf{q}) = \bar{Q}_1 \bar{Q}_2 [I \ \mathbf{q}I \ \dots \ \mathbf{q}^{d_1+d_2} I]^\top, \quad (24)$$

where

$$\bar{Q}_1 = \begin{bmatrix} Q_{1,0} & Q_{1,1} & \cdots & Q_{1,d_1} \end{bmatrix},$$

$$\bar{Q}_2 = \begin{bmatrix} Q_{2,0} & Q_{2,1} & \cdots & Q_{2,d_2} & 0 & \cdots & 0 \\ 0 & Q_{2,0} & Q_{2,1} & \cdots & Q_{2,d_2} & 0 & \vdots \\ \vdots & & \ddots & \ddots & & \ddots & 0 \\ 0 & 0 & \cdots & Q_{2,0} & Q_{2,1} & \cdots & Q_{2,d_2} \end{bmatrix}.$$

Lemma 4.2. (\mathcal{H}_2 -norm [33, Lemma 1]) Consider the linear time-invariant discrete-time system

$$\begin{aligned} x(k+1) &= Ax(k) + B\omega(k), \\ y(k) &= Cx(k), \end{aligned}$$

where the state $x \in \mathbb{R}^{n_x}$ and all other vectors and matrices have appropriate dimensions. Let $\mathbf{T}_{\omega y}$ denote the transfer function from ω to y . For a constant $\eta \in \mathbb{R}_{>0}$, A is stable and the \mathcal{H}_2 -norm of $\mathbf{T}_{\omega y}$ satisfies $\|\mathbf{T}_{\omega y}\|_2^2 \leq \eta$ if and only if there exists matrices $P, Z \in \mathcal{S}_+$ such that the following LMIs are feasible

$$\begin{bmatrix} P & AP & B \\ * & P & 0 \\ * & * & I \end{bmatrix} \succeq 0, \quad \begin{bmatrix} Z & CP \\ * & P \end{bmatrix} \succeq 0, \quad \text{Trace}(Z) \leq \eta.$$

Proof of Theorem 3.1. First, we show that the equality (15a) guarantees the satisfaction of the property (3a). According to Lemma 4.1, we have

$$N_{ij}(\mathbf{q})H_{ij}(\mathbf{q}) = \bar{N}_{ij}\bar{H}_{ij}[I \ \mathbf{q}I \ \cdots \ \mathbf{q}^{d_N+1}I]^\top.$$

Hence, (15a) implies that $N_{ij}(\mathbf{q})H_{ij}(\mathbf{q}) = 0$. The contribution of d in r_{ij} is completely canceled when the status is \mathcal{S}_{ij} (as shown in (11)). This concludes the first part of the proof.

In the second part of the proof, we show that the inequalities (15b) imply the satisfaction of the property (3b). Suppose that the status is \mathcal{S}_{ih} for $h \in [n]/\{j\}$. According to the closed-loop dynamics (7), we have

$$y(k) = C_h(\mathbf{q}I - A_{ih}^{cl})^{-1}[E_h d(k) + B_h K_i D\omega(k)] + D\omega(k).$$

By virtue of (11), the transfer function $\mathbf{T}_{dr_{ij}}^{\mathcal{S}_{ih}}(\mathbf{q})$ is written as

$$\begin{aligned} \mathbf{T}_{dr_{ij}}^{\mathcal{S}_{ih}}(\mathbf{q}) &= \frac{N_{ij}(\mathbf{q})L(\mathbf{q})}{a(\mathbf{q})} C_h(\mathbf{q}I - A_{ih}^{cl})^{-1} E_h \\ &= a^{-1}(\mathbf{q}) \bar{N}_{ij} \bar{L} [I \ \mathbf{q}I \ \cdots \ \mathbf{q}^{d_N} I]^\top C_h(\mathbf{q}I - A_{ih}^{cl})^{-1} E_h, \end{aligned}$$

where Lemma 4.1 is used in the second equality. Then, we enforce the ℓ_∞ norm of the steady-state gain of $\mathbf{T}_{dr_{ij}}^{\mathcal{S}_{ih}}(\mathbf{q})$ to be larger than or equal to 1, which is

$$\left\| \mathbf{T}_{dr_{ij}}^{\mathcal{S}_{ih}}(1) \right\|_\infty = \|a^{-1}(1) \bar{N}_{ij} \bar{L} \mathcal{L}_{ih}\|_\infty \geq 1.$$

Thanks to the linearity of the deigned filters, one can scale (15b) and get (3b). This concludes the second part of the proof.

In the third part, we show that the inequalities (15c) and (15d) enforce the desired property (3c). When the status is S_{ij} , from (11), the transfer function from ω to r_{ij} is

$$\mathbf{T}_{\omega r_{ij}}^{S_{ij}}(\mathbf{q}) = -\frac{N_{ij}(\mathbf{q})G_{ij}(\mathbf{q})}{a(\mathbf{q})}. \quad (25)$$

The observable canonical realization of (25) is $(A_r, B_{\omega r_{ij}}^{S_{ij}}, C_r)$. According to Lemma 4.2, the inequality (15c) directly implies $\|\mathbf{T}_{\omega r_{ij}}^{S_{ij}}\|_2^2 \leq \eta_{ij}^{S_{ij}}$. When the status is S_{ih} for $h \in [n]/\{j\}$, the transfer function from ω to r_{ij} can be obtained from (14). Again, the inequalities (15d) imply $\|\mathbf{T}_{\omega r_{ij}}^{S_{ih}}\|_2^2 \leq \eta_{ij}^{S_{ih}}$ by applying Lemma 4.2. Then we minimize the sum of $\eta_{ij}^{S_{im}}$ for all $m \in [n]$ to suppress the effect of the noise on r_{ij} . This completes the proof. \square

Proof of Proposition 3.2. This proof is to show that (16) ensures the satisfaction of the nonlinear matrix inequality in (15d). By applying Schur complement to (16), we have

$$\begin{aligned} & \begin{bmatrix} P_{ij}^{S_{ih}} & \hat{A}_{ih}G_{ij}^{S_{ih}} \\ * & \Xi_{ij}^{S_{ih}} \end{bmatrix} - \begin{bmatrix} \hat{B}_{r_{ij}} & 0 \\ * & (\hat{D}_hG_{ij}^{S_{ih}})^\top \end{bmatrix} \begin{bmatrix} \gamma I & 0 \\ * & \frac{1}{\gamma} I \end{bmatrix} \begin{bmatrix} \hat{B}_{r_{ij}}^\top & 0 \\ * & \hat{D}_hG_{ij}^{S_{ih}} \end{bmatrix} \\ & = \begin{bmatrix} P_{ij}^{S_{ih}} & \hat{A}_{ih}G_{ij}^{S_{ih}} \\ * & \Xi_{ij}^{S_{ih}} \end{bmatrix} - \gamma \begin{bmatrix} \hat{B}_{r_{ij}} \\ 0 \end{bmatrix} \begin{bmatrix} \hat{B}_{r_{ij}}^\top & 0 \end{bmatrix} - \frac{1}{\gamma} \begin{bmatrix} 0 \\ (\hat{D}_hG_{ij}^{S_{ih}})^\top \end{bmatrix} \begin{bmatrix} 0 & \hat{D}_hG_{ij}^{S_{ih}} \end{bmatrix} \succeq 0. \end{aligned} \quad (26)$$

Note that, for matrices A, B with appropriate dimensions and any scalar $\gamma > 0$, it holds that $\gamma AA^\top + \frac{1}{\gamma} B^\top B \succeq AB + B^\top A^\top$ [29, Lemma 1]. We have

$$\begin{aligned} & - \begin{bmatrix} \hat{B}_{r_{ij}} \\ 0 \end{bmatrix} \begin{bmatrix} 0 & \hat{D}_hG_{ij}^{S_{ih}} \end{bmatrix} - \begin{bmatrix} 0 \\ (\hat{D}_hG_{ij}^{S_{ih}})^\top \end{bmatrix} \begin{bmatrix} \hat{B}_{r_{ij}}^\top & 0 \end{bmatrix} \\ & \succeq - \gamma \begin{bmatrix} \hat{B}_{r_{ij}} \\ 0 \end{bmatrix} \begin{bmatrix} \hat{B}_{r_{ij}}^\top & 0 \end{bmatrix} - \frac{1}{\gamma} \begin{bmatrix} 0 \\ (\hat{D}_hG_{ij}^{S_{ih}})^\top \end{bmatrix} \begin{bmatrix} 0 & \hat{D}_hG_{ij}^{S_{ih}} \end{bmatrix}. \end{aligned} \quad (27)$$

Thus, the inequality (26) can be written as

$$\begin{aligned} & \begin{bmatrix} P_{ij}^{S_{ih}} & \hat{A}_{ih}G_{ij}^{S_{ih}} \\ * & \Xi_{ij}^{S_{ih}} \end{bmatrix} - \begin{bmatrix} \hat{B}_{r_{ij}} \\ 0 \end{bmatrix} \begin{bmatrix} 0 & \hat{D}_hG_{ij}^{S_{ih}} \end{bmatrix} - \begin{bmatrix} 0 \\ (\hat{D}_hG_{ij}^{S_{ih}})^\top \end{bmatrix} \begin{bmatrix} \hat{B}_{r_{ij}}^\top & 0 \end{bmatrix} \\ & = \begin{bmatrix} P_{ij}^{S_{ih}} & \hat{A}_{ih}G_{ij}^{S_{ih}} - \hat{B}_{r_{ij}}\hat{D}_hG_{ij}^{S_{ih}} \\ * & \Xi_{ij}^{S_{ih}} \end{bmatrix} \succeq 0. \end{aligned} \quad (28)$$

By expanding $\hat{A}_{ih}G_{ij}^{S_{ih}} - \hat{B}_{r_{ij}}\hat{D}_hG_{ij}^{S_{ih}}$, we have

$$\begin{aligned} & \begin{bmatrix} A_{ih}^{cl} & 0 \\ 0 & A_r \end{bmatrix} G_{ij,1}^{S_{ih}} \begin{bmatrix} B_hK_iD \\ 0 \end{bmatrix} G_{ij,2}^{S_{ih}} - \begin{bmatrix} 0 \\ -B_{r_{ij}} \end{bmatrix} \begin{bmatrix} C_h & 0 \end{bmatrix} G_{ij,1}^{S_{ih}} \begin{bmatrix} 0 \\ -B_{r_{ij}} \end{bmatrix} DG_{ij,2}^{S_{ih}} \\ & = \begin{bmatrix} A_{ih}^{cl} & 0 \\ B_{r_{ij}}C_h & A_r \end{bmatrix} G_{ij,1}^{S_{ih}} \begin{bmatrix} B_hK_iD \\ B_{r_{ij}}D \end{bmatrix} G_{ij,2}^{S_{ih}} \\ & = \begin{bmatrix} \tilde{A}_{ij}^{S_{ih}} & \tilde{D}_{ij}^{S_{ih}} \end{bmatrix} G_{ij}^{S_{ih}}. \end{aligned} \quad (29)$$

From (29), the inequality (28) is equivalent to

$$\begin{bmatrix} P_{ij}^{S_{ih}} & \begin{bmatrix} \tilde{A}_{ij}^{S_{ih}} & \tilde{D}_{ij}^{S_{ih}} \end{bmatrix} G_{ij}^{S_{ih}} \\ * & \Xi_{ij}^{S_{ih}} \end{bmatrix} \succeq 0. \quad (30)$$

For a scalar $\alpha \in \mathbb{R}$, matrices A, B with appropriate dimensions, and $A \succeq 0$, note that $(B - \alpha A)^\top A^{-1} (B - \alpha A) \succeq 0$ implies $B^\top A^{-1} B \succeq \alpha B + \alpha B^\top - \alpha^2 A$. Thus, we have

$$G_{ij}^{S_{ih} \top} \begin{bmatrix} P_{ij}^{S_{ih}} & 0 \\ * & I \end{bmatrix}^{-1} G_{ij}^{S_{ih}} \succeq \Xi_{ij}^{S_{ih}}. \quad (31)$$

By combining (30) and (31), we obtain that

$$\begin{bmatrix} P_{ij}^{S_{ih}} & \begin{bmatrix} \tilde{A}_{ij}^{S_{ih}} & \tilde{D}_{ij}^{S_{ih}} \end{bmatrix} G_{ij}^{S_{ih}} \\ * & G_{ij}^{S_{ih} \top} \begin{bmatrix} P_{ij}^{S_{ih}} & 0 \\ * & I \end{bmatrix}^{-1} G_{ij}^{S_{ih}} \end{bmatrix} \succeq 0. \quad (32)$$

Pre- and post-multiplying (32) by $\text{diag}(I, G_{ij}^{S_{ih} \top})^{-1}$ and $\text{diag}(I, P_{ij}^{S_{ih}}, I)$ and their transpose successively, we arrive at

$$\begin{bmatrix} P_{ij}^{S_{ih}} & \tilde{A}_{ij}^{S_{ih}} P_{ij}^{S_{ih}} & \tilde{D}_{ij}^{S_{ih}} \\ * & P_{ij}^{S_{ih}} & 0 \\ * & * & I \end{bmatrix} \succeq 0. \quad (33)$$

This completes the proof. \square

Proof of Proposition 3.3. We first show that the inequality (17a) is a necessary and sufficient condition for the equation (15a) having non-trivial solutions. According to Rank Plus Nullity Theorem [34, Chapter 4], it holds that $(d_N + 1)(n_x + n_y) = \text{Rank}(\bar{H}_{ij}) + \text{Null}(\bar{H}_{ij})$, where $\text{Null}(\bar{H}_{ij})$ denotes the dimension of the left null space of \bar{H}_{ij} . Thus, (15a) having non-trivial solutions is equivalent to $\text{Null}(\bar{H}_{ij})$ being nonzero. This concludes the first part of the proof.

Second, we show that (17b) is equivalent to (15b) when (17a) holds. (\Rightarrow) We proceed the proof by contradiction. Suppose that (15b) holds but (17b) is not satisfied, we have $\text{Rank}([\bar{H}_{ij} \ \mathcal{L}_{ih}]) = \text{Rank}(\bar{H}_{ij})$. This means that \mathcal{L}_{ih} belongs to the column range space of \bar{H}_{ij} . In other words, there exists a vector $\xi \in \mathbb{R}^{(n_x + n_d)(d_N + 2)}$, such that $\mathcal{L}_{ih} = \bar{H}_{ij} \xi$. Since \bar{N}_{ij} satisfying $\bar{N}_{ij} \bar{H}_{ij} = 0$, we have $\bar{N}_{ij} \mathcal{L}_{ih} = \bar{N}_{ij} \bar{H}_{ij} \xi = 0$, which contradicts to (15b). (\Leftarrow) Assume that (17b) holds. This means that the left null space of \bar{H}_{ij} and \mathcal{L}_{ih} are not the same. Thus, one can find a \bar{N}_{ij} which satisfies (15a) and (15b) at the same time. This completes the second part of the proof.

Finally, it is known from Lemma 4.2 that $|\Lambda(A_r)| < 1$, and $|\Lambda(\tilde{A}_{ij}^{S_{ih}})| < 1$ are necessary and sufficient conditions for the feasibility of (15c) and (15d), resp. Recalling the definition of $\tilde{A}_{ij}^{S_{ih}}$ in (14), $|\Lambda(\tilde{A}_{ij}^{S_{ih}})| < 1$ if and only if $|\Lambda(A_r)| < 1$ and $|\Lambda(A_{ih}^{cl})| < 1$. This completes the proof. \square

4.2. Proofs of probabilistic certificates

In order to prove Theorem 3.6, we introduce the following lemma.

Lemma 4.3 (Linear transformation of sub-Gaussian variables). *Suppose $\mathbf{T}_{\omega r}(\mathbf{q})$ is the transfer function from ω to r , i.e., $r(k) = \mathbf{T}_{\omega r}(\mathbf{q})\omega(k)$, with the state-space realization (A, B, C) . If the input ω is i.i.d sub-Gaussian signal with zero mean and parameter \mathcal{C}_ω , the output r is also sub-Gaussian and its parameter equals to $\mathcal{C}_r = \|\mathbf{T}_{\omega r}(\mathbf{q})\|_2 \mathcal{C}_\omega$.*

Proof. The deviation of $r(k)$ from $\mathbf{E}[r(k)]$ can be computed by $r(k) - \mathbf{E}[r(k)] = C \sum_{m=0}^{k-1} A^{k-1-m} B \omega(m)$. Then, for any constant ϕ and unit vector ν , we have

$$\begin{aligned} \mathbf{E} \left[e^{\phi \nu^\top (r(k) - \mathbf{E}[r(k)])} \right] &= \mathbf{E} \left[e^{\phi \nu^\top C \sum_{m=0}^{k-1} A^{k-1-m} B \omega(m)} \right] \\ &= \prod_{m=0}^{k-1-m} \mathbf{E} \left[e^{\phi \nu^\top C A^{k-1-m} B \omega(m)} \right], \end{aligned} \quad (34)$$

Since ω is sub-Gaussian, according to Lemma 3.4, it holds that

$$\mathbf{E} \left[e^{\phi \nu^\top C A^{k-1-m} B \omega(m)} \right] \leq e^{\phi^2 \|\nu^\top\|_2^2 \|C A^{k-1-m} B\|_2^2 \mathcal{C}_\omega^2 / 2}. \quad (35)$$

Recall that $\|\nu\|_2 = 1$. Thus, equality (34) satisfies the following inequality

$$\begin{aligned} \mathbf{E} \left[e^{\phi \nu^\top (r(k) - \mathbf{E}[r(k)])} \right] &\leq \prod_{m=0}^{k-1-m} e^{\phi^2 \|C A^{k-1-m} B\|_2^2 \mathcal{C}_\omega^2 / 2} \\ &= e^{\phi^2 \sum_{m=0}^{k-1-m} \|C A^{k-1-m} B\|_2^2 \mathcal{C}_\omega^2 / 2}. \end{aligned} \quad (36)$$

According to the property of matrix norm, it holds that $\|A\|_2^2 \leq \text{Trace}(A^\top A)$ for all real matrix A , where $\text{Trace}(\cdot)$ denotes the trace of a matrix. We have

$$\begin{aligned} \mathbf{E} \left[e^{\phi \nu^\top (r(k) - \mathbf{E}[r(k)])} \right] &\leq e^{\phi^2 \sum_{m=0}^{k-1-m} \text{Trace}(C A^{k-1-m} B B^\top A^{\top k-1-m} C^\top)} \mathcal{C}_\omega^2 / 2 \\ &\leq e^{\phi^2 \|\mathbf{T}_{\omega r}(\mathbf{q})\|_2^2 \mathcal{C}_\omega^2 / 2}. \end{aligned} \quad (37)$$

where we use Parseval's Theorem and the definition of \mathcal{H}_2 norm of a transfer function in the last inequality. This completes the proof. \square

Proof of Theorem 3.6. The main idea builds on the probabilistic relation between the concentration of a random variable and its expectation. First, according to Lemma 4.3, the matched residual r_{ij} is sub-Gaussian with parameter satisfying $\|\mathbf{T}_{\omega r_{ij}}^{S_{ij}}\|_2 \leq \sqrt{\bar{\eta}_i}$ because the noise ω is sub-Gaussian. When the expected value $|\mathbf{E}[r_{ij}(k)]| \leq \mu \sqrt{\bar{\eta}_i} = \varepsilon_i - \sqrt{2 \ln(2/\beta) \bar{\eta}_i}$, we have

$$\begin{aligned} \Pr \left[|r_{ij}(k)| \leq \varepsilon_i \mid \mathbf{M}_{i \rightarrow j}^{t_s} \right] &= \Pr \left[|r_{ij}(k)| - |\mathbf{E}[r_{ij}(k)]| \leq \varepsilon_i - |\mathbf{E}[r_{ij}(k)]| \mid \mathbf{M}_{i \rightarrow j}^{t_s} \right] \\ &\geq \Pr \left[|r_{ij}(k) - \mathbf{E}[r_{ij}(k)]| \leq \sqrt{2 \ln(2/\beta) \bar{\eta}_i} \mid \mathbf{M}_{i \rightarrow j}^{t_s} \right] \\ &\geq 1 - 2e^{-\ln(2/\beta) \bar{\eta}_i / \|\mathbf{T}_{\omega r_{ij}}^{S_{ij}}(\mathbf{q})\|_2^2} \geq 1 - \beta. \end{aligned} \quad (38)$$

The first inequality in (38) holds because $|r_{ij}(k)| - |\mathbf{E}[r_{ij}(k)]| \leq |r_{ij}(k) - \mathbf{E}[r_{ij}(k)]|$. We use the concentration inequality (18) in Lemma 3.4 and get the second inequality.

Next, we show that $|\mathbf{E}[r_{ij}(k)]| \leq \mu \sqrt{\bar{\eta}_i}$ when $k \geq t_s + T_{ij}$. Note that $|\mathbf{E}[r_{ij}]|$ is above the threshold because the system state is nonzero at t_s , i.e., $x(t_s) \neq 0$. Hence, let us compute the expression

of $\mathbf{E}[r_{ij}(k)]$ with $x(t_s)$. The state $x(t_s)$ is viewed as an input to the system that only has a nonzero value at t_s . The closed-loop dynamics (7) for $k = t_s + \Delta k$ where $\Delta k \in [0, t_{\text{iso}}^s)$ becomes

$$\begin{aligned} x(k+1) &= A_{ij}^{cl}x(k) + E_j d(k) + B_j K_i D \omega(k) + x(t_s), \\ y(k) &= C_j x(k) + D \omega(k). \end{aligned} \quad (39)$$

We reformulate (39) into the DAE format, which is

$$\begin{bmatrix} -\mathbf{q}I + A_{ij}^{cl} & E_j & I \\ C_j & 0 & 0 \end{bmatrix} \begin{bmatrix} x(k) \\ d(k) \\ x(t_s) \end{bmatrix} + L(\mathbf{q})y(k) + G_{ij}(\mathbf{q})\omega(k) = 0. \quad (40)$$

Multiplying from left of (40) by $a^{-1}(\mathbf{q})N_{ij}(\mathbf{q})$ leads to

$$r_{ij}(k) = \frac{N_{ij}(\mathbf{q})L(\mathbf{q})}{a(\mathbf{q})}y(k) = -\frac{N_{ij}(\mathbf{q})}{a(\mathbf{q})} \begin{bmatrix} -\mathbf{q}I + A_{ij}^{cl} & E_j & I \\ C_j & 0 & 0 \end{bmatrix} \begin{bmatrix} x(k) \\ d(k) \\ x(t_s) \end{bmatrix} - \frac{N_{ij}(\mathbf{q})G_{ij}(\mathbf{q})}{a(\mathbf{q})}\omega(k). \quad (41)$$

Recall from Theorem 3.1 that $N_{ij}(\mathbf{q})H_{ij}(\mathbf{q}) = 0$, and substitute $N_{ij}(\mathbf{q}) = [\hat{N}_{ij}(\mathbf{q}) \check{N}_{ij}(\mathbf{q})]$ into (41). We have

$$r_{ij}(k) = -\frac{\hat{N}_{ij}(\mathbf{q})}{a(\mathbf{q})}x(t_s) - \frac{N_{ij}(\mathbf{q})G_{ij}(\mathbf{q})}{a(\mathbf{q})}\omega(k). \quad (42)$$

Hence, the expected value of $r_{ij}(k)$ is

$$\mathbf{E}[r_{ij}(k)] = -a^{-1}(\mathbf{q})\hat{N}_{ij}(\mathbf{q})\mathbf{E}[x(t_s)]. \quad (43)$$

To compute T_{ij} , following the idea of [35, Lemma 3.4], we transform $-a^{-1}(\mathbf{q})\hat{N}_{ij}(\mathbf{q})$ to its Jordan canonical form denoted by $(\bar{A}_r, \bar{B}_{r_{ij}}, \bar{C}_r)$. The transfer function $-a^{-1}(\mathbf{q})\hat{N}_{ij}(\mathbf{q})$ can be expanded as

$$-\frac{\hat{N}_{ij}(\mathbf{q})}{a(\mathbf{q})} = \left[-\frac{\sum_{m=0}^{d_N} \hat{N}_{ij,m}(1)\mathbf{q}^m}{a(\mathbf{q})}, \dots, -\frac{\sum_{m=0}^{d_N} \hat{N}_{ij,m}(n_x)\mathbf{q}^m}{a(\mathbf{q})} \right],$$

Recall that $a(\mathbf{q}) = \prod_{l=1}^{d_N+1} (\mathbf{q} - \lambda_l)$. The factorization of the h -th element of $-a^{-1}(\mathbf{q})\hat{N}_{ij}(\mathbf{q})$ is

$$-\frac{\sum_{m=0}^{d_N} \hat{N}_{ij,m}(h)\mathbf{q}^m}{a(\mathbf{q})} = \sum_{l=1}^{d_N+1} \frac{b_{ij,th}}{\mathbf{q} - \lambda_l},$$

where $b_{ij,th} = -\frac{\sum_{m=0}^{d_N} \hat{N}_{ij,m}(h)\lambda_l^m}{\prod_{i \neq l} (\lambda_i - \lambda_l)}$. The Jordan canonical form of $-a^{-1}(\mathbf{q})\sum_{m=0}^{d_N} \hat{N}_{ij,m}(h)\mathbf{q}^m$ is denoted by $(\bar{A}_{r,h}, \bar{B}_{r_{ij},h}, \bar{C}_{r,h})$, where

$$\bar{A}_{r,h} = \text{diag}([\lambda_1, \dots, \lambda_{d_N+1}]), \quad \bar{B}_{r_{ij},h} = [b_{ij,1h}, \dots, b_{ij,(d_N+1)h}]^\top, \quad \bar{C}_{r,h} = [1, \dots, 1].$$

Then, according to the superposition property of linear systems, we have

$$\bar{A}_r = \text{diag}([\lambda_1, \dots, \lambda_{d_N+1}]), \quad \bar{B}_{r_{ij}} = [\bar{B}_{r_{ij},1}, \dots, \bar{B}_{r_{ij},n_x}], \quad \bar{C}_r = [1, \dots, 1].$$

With the state-space description, $\mathbf{E}[r_{ij}(k)]$ can be written as

$$\begin{aligned} \mathbf{E}[r_{ij}(k)] &= \bar{C}_r \bar{A}_r^{\Delta k} \mathbf{E}[\bar{x}_{ij}(t_s)] + \bar{C}_r \sum_{m=0}^{\Delta k-1} \bar{A}_r^{\Delta k-1-m} \bar{B}_{r_{ij}} \mathbf{E}[x(t_s)] \\ &= \bar{C}_r \bar{A}_r^{\Delta k} \mathbf{E}[\bar{x}_{ij}(t_s)] + \bar{C}_r \bar{A}_r^{\Delta k-1} \bar{B}_{r_{ij}} \mathbf{E}[x(t_s)], \end{aligned} \quad (44)$$

where $\tilde{x}_{ij}(t_s)$ is the state of the filter. Since \bar{A}_r is a diagonal matrix, we have $\|\bar{A}_r\|_2 = \lambda_{\max}$. Based on the triangle property of norms, $|\mathbf{E}[r_{ij}(k)]|$ is bounded by

$$\begin{aligned} |\mathbf{E}[r_{ij}(k)]| &\leq \|\bar{C}_r\|_2 \|\bar{A}_r\|_2^{\Delta k} \|\mathbf{E}[\tilde{x}_{ij}(t_s)]\|_2 + \|\bar{C}_r\|_2 \|\bar{A}_r\|_2^{\Delta k-1} \|\bar{B}_{r_{ij}}\|_2 \|\mathbf{E}[x(t_s)]\|_2 \\ &\leq \sqrt{d_N + 1} (1 + \lambda_{\max}^{-1} \|\bar{B}_{r_{ij}}\|_2) \|\mathbf{E}[\tilde{x}_{ij}(t_s)]\|_2 \lambda_{\max}^{\Delta k} = \psi_{ij}(\mathbf{F}_{ij}, \tilde{x}_{ij}(t_s)) \lambda_{\max}^{\Delta k}. \end{aligned} \quad (45)$$

By setting $\mu\sqrt{\eta_i} \geq \psi_{ij}(\mathbf{F}_{ij}, \tilde{x}_{ij}(t_s)) \lambda_{\max}^{\Delta k}$, we arrive at

$$\Delta k \geq T_{ij} = \left\lceil \log_{\lambda_{\max}} \frac{\mu\sqrt{\eta_i}}{\psi_{ij}(\mathbf{F}_{ij}, \tilde{x}_{ij}(t_s))} \right\rceil.$$

That completes the proof. \square

5. ILLUSTRATIVE EXAMPLES

In this section, we consider a numerical example and a practical application on building radiant systems to illustrate the effectiveness of the proposed approach.

5.1. Numerical results

Consider a switched system with three linear subsystems. The system matrices are

$$\begin{aligned} A_1 &= \begin{bmatrix} 0.3 & -0.05 \\ 0.12 & -0.3 \end{bmatrix}, A_2 = \begin{bmatrix} 0.51 & -0.24 \\ 0.80 & 0.32 \end{bmatrix}, A_3 = \begin{bmatrix} -0.50 & 0.16 \\ 0.80 & 0.64 \end{bmatrix}, B_1 = B_2 = B_3 = \begin{bmatrix} 1 \\ 1 \end{bmatrix}, D = \begin{bmatrix} 0.001 & 0 \\ 0.001 & -0.001 \end{bmatrix} \\ E_1 &= \begin{bmatrix} 0.7 \\ 1.3 \end{bmatrix}, E_2 = \begin{bmatrix} 0.2 \\ -1.4 \end{bmatrix}, E_3 = \begin{bmatrix} -1.1 \\ 0.9 \end{bmatrix}, C_1 = \begin{bmatrix} 0.2 & 0 \\ 0.1 & 0.15 \end{bmatrix}, C_2 = \begin{bmatrix} 0.3 & 0.4 \\ 0.1 & -0.2 \end{bmatrix}, C_3 = \begin{bmatrix} -0.1 & 0.2 \\ 0.4 & 0.1 \end{bmatrix}. \end{aligned}$$

The controller gains are $K_1 = [-0.1335 \ -0.0041]$, $K_2 = [-0.2095 \ -0.2692]$, and $K_3 = [-0.1668 \ -0.0632]$. We set the degree of the filters $d_N = 1$, the denominator $a(q) = (q + 0.1)(q + 0.2)$. The reference signal is set as $\bar{d} = 0.3$. The parameter of the i.i.d sub-Gaussian noise is 1. The filters are constructed by using the approach proposed in Theorem 3.1 and Proposition 3.2. We solve the optimization problems by YALMIP toolbox [36]. The thresholds are computed according to (19) where the reliability level $\beta = 0.05$ and $\mu = 0.5$. Thus, the thresholds are $\varepsilon_1 = 0.18$, $\varepsilon_2 = 0.12$, $\varepsilon_3 = 0.17$. The waiting time τ_i for $i \in [3]$ computed by (21) are $\tau_1 = 5$, $\tau_2 = 6$, $\tau_3 = 7$. To cover all the scenarios, we set the switching sequence as: $1 \rightarrow 2 \rightarrow 3 \rightarrow 1 \rightarrow 3 \rightarrow 2 \rightarrow 1$. Figure 4 shows the diagnosis result of the whole process, where the switching signal is correctly estimated.

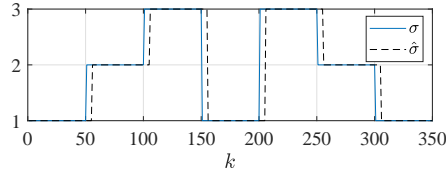


FIGURE 4. Diagnosis result of the whole process

Figure 5 depicts the residuals behavior under different scenarios. Here, we only analyze r_{1h} for $h \in [3]$ with the transition M_{12}^{50} shown in Figure 5(a), because the rest are similar. Since the initial status of the closed-loop system is S_{11} , the residual r_{11} remains below ε_1 until transition happens at $k = 50$. The other two residuals r_{12} and r_{13} first reach their corresponding steady values, and then oscillate around the steady values because of the noise. The matched residual r_{11} and the

unmatched residuals r_{12} and r_{13} are separated. After the transition M_{12} happens at $k = 50$, r_{11} exceeds the threshold ε_1 immediately such that the switching is detected. Then, r_{12} reaches ε_1 at about $k = 55$ while the other two residuals are above ε_1 . As a result, active mode 2 is determined.

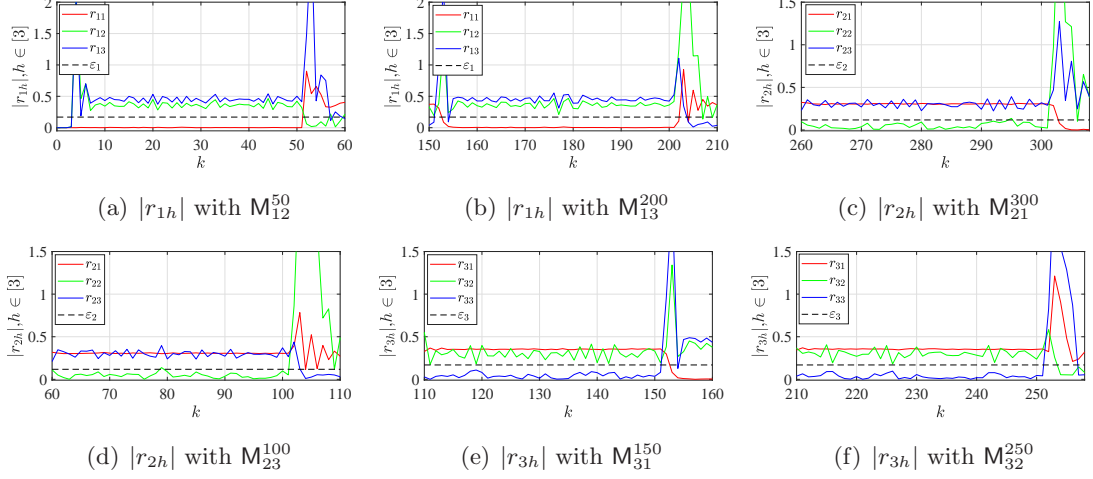


FIGURE 5. Residuals behavior under different scenarios: We recall that M_{ij}^k stands for a system transition from i to j at time k .

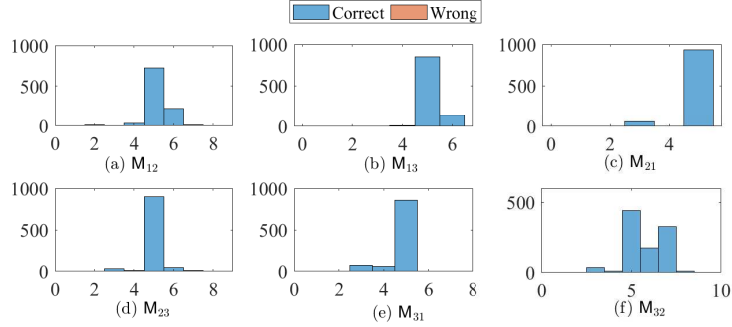


FIGURE 6. Distribution of the diagnosis time for each scenario

We execute the experiment 1000 times for each switching scenario to obtain the distribution of the diagnosis time as well as the probability of wrong detection. The results are shown in Figure 6. The average diagnosis time (ADT) and the wrong detection probability (WDP) are presented in Table 1. We compute the estimated matched time T_{ij} based on (20). From Table 1, we can see that the estimated matched time estimates the average diagnosis time well, and the wrong detection probability is low.

TABLE 1. Average diagnosis time and wrong detection probability when $\mu = 0.5$ and $\beta = 0.05$

Transition	M_{12}	M_{13}	M_{21}	M_{23}	M_{31}	M_{32}
ADT	6	6	5	5	5	6
T_{ij}	7	7	5	6	5	7
WDP	0.001	0	0	0.004	0.001	0

5.2. Building radiant systems

In this section, a building radiant system is considered to illustrate the performance of the proposed approach. We adopt the example from [37], where the building with four rooms of the same size is equipped with a radiant system with two pumps. Moreover, we compare the model invalidation approach proposed in [37] with our diagnosis approach.

5.2.1. *System model description.* The radiant system can then be modelled by the following equations

$$\begin{aligned}
C_{c,1}\dot{T}_{c,1} &= K_{c,1}(T_1 - T_{c,1}) + K_{c,3}(T_3 - T_{c,1}) + K_{w,1}(T_{w,1} - T_{c,1}), \\
C_{c,2}\dot{T}_{c,2} &= K_{c,2}(T_2 - T_{c,2}) + K_{c,4}(T_4 - T_{c,2}) + K_{w,2}(T_{w,2} - T_{c,2}), \\
C_1\dot{T}_1 &= K_{c,1}(T_{c,1} - T_1) + K_1(T_a - T_1) + K_{12}(T_2 - T_1) + K_{13}(T_3 - T_1), \\
C_2\dot{T}_2 &= K_{c,2}(T_{c,2} - T_2) + K_2(T_a - T_2) + K_{12}(T_1 - T_2) + K_{24}(T_4 - T_2), \\
C_3\dot{T}_3 &= K_{c,1}(T_{c,1} - T_3) + K_3(T_a - T_3) + K_{13}(T_1 - T_3) + K_{34}(T_4 - T_3), \\
C_2\dot{T}_4 &= K_{c,2}(T_{c,2} - T_4) + K_4(T_a - T_4) + K_{24}(T_2 - T_4) + K_{34}(T_3 - T_4),
\end{aligned}$$

where the temperature of two cores in the radiant system is denoted by $T_{c,i}$ for $i \in [2]$. The temperature of the supply water is denoted by $T_{w,i}$. The ambient air temperature is denoted by T_a . The air temperature of room i for $i \in [4]$ is denoted by T_i . The thermal conductance between T_i and T_a is denoted by K_i . The thermal conductance between $T_{c,i}$ and T_i is denoted by $K_{c,i}$. The thermal conductance between room i and j is denoted by K_{ij} . The piping thermal conductance between $T_{c,i}$ and $T_{w,i}$ is denoted by $K_{w,i}$. The thermal capacitance of room i and core i is denoted by C_i and $C_{c,i}$, resp. Assume that the constant flow of pumps is known. Each pump supplies water to the water pipe and is connected to a valve to adjust the constant flow. The states of the system are the temperatures of the four rooms and the two cores. Suppose both pumps are on. The values of the parameters are the same as that in [37]. The above equations can be written into the state-space form

$$\begin{aligned}
\dot{x}_T &= A_{rad,1}x_T + E_{rad,1}T_d, \\
y &= C_{rad,1}x_T + \omega
\end{aligned} \tag{46}$$

where $x_T := [T_{c,1}, T_{c,2}, T_1, T_2, T_3, T_4]^\top$ is state, $T_d := [T_{w,1}, T_{w,2}, T_a]^\top$ is a constant input (or reference signal). Matrices $A_{rad,1}$ and $E_{rad,1}$ are obtained from the above equations. The matrix $C_{rad,1} = \text{diag}([0, 0, 1, 1, 1, 1])$ indicates the measured states. Assume there is an uncertainty ν in T_a due to small changes (i.e., $T_a = 10 + \nu$ with $\nu \sim \mathcal{N}(0, 0.1)$). The measurement noise is denoted by ω and subjects to $\mathcal{N}(0, 0.01)$. The discrete-time model of the radiant system (46) is obtained with sampling time of 5 min. Let $(A_{rad,1}^d, E_{rad,1}^d, C_{rad,1})$ represents the fault-free discrete-time model of the system.

5.2.2. *Faulty modes.* The normal functions of the valves and temperature measurement sensors are impaired in the faulty modes. Specifically, when there is a fault in the valve, we assume that the valve is stuck in the middle and does not respond to commands. Since the fault cuts the heat transfer in half, the fault is modelled with a change in the heat conductance parameter, i.e., $K_{w,1} \rightarrow K_{w,1}/2$

in $A_{rad,1}$ and $E_{rad,1}$. The sensor failures result in inaccurate measurements of the temperature. We change the corresponding entry in $C_{rad,1}$ to model the sensor fault, i.e., $1 \rightarrow 0.9$. Here, two faulty modes are considered. The first faulty mode is denoted by $(A_{rad,2}^d, E_{rad,2}^d, C_{rad,2})$, where faults occur in the second pump and the sensor measuring T_1 . As a result, $K_{w,2}$ decreases to $K_{w,2}/2$ and $C_{rad,2} = \text{diag}([0, 0, 0.9, 1, 1, 1])$. The second faulty mode is denoted by $(A_{rad,3}^d, E_{rad,3}^d, C_{rad,3})$, where fault only occurs in the first pump. Note that the second faulty mode is more incipient than the first one because the outputs do not change dramatically. The matched residual of $(A_{rad,i}^d, E_{rad,i}^d, C_{rad,i})$ is defined as r_i for $i \in [3]$.

5.2.3. Filter design and model invalidation approach. Note that there is no control signal in the radiant system (46). Thus, we only need to design 3 filters corresponding to the 3 modes. The degree of the filters is set as $d_N = 3$. The filters are then constructed based on Theorem 3.1 and Proposition 3.2. The idea of the model invalidation approach proposed in [37] is that given the input and output data, detect the transitions by checking the feasibility of a mixed integer linear programming (MILP) problem. Since the example we adopt here has only one healthy mode, the MILP problem degenerates into the following linear programming problem.

$$\begin{aligned} & \text{Find } \mathbf{x}(k), \boldsymbol{\nu}(k), \boldsymbol{\omega}(k), \forall k \in \{0, 1, \dots, T-1\} \\ & \text{s.t. } \begin{cases} \mathbf{x}(k+1) - A_{rad,1}\mathbf{x}(k) - E_{rad,1}(T_d + [0, 0, \boldsymbol{\nu}(k)]^\top) = 0, \\ y(k) - C_{rad,1}\mathbf{x}(k) - \boldsymbol{\omega}(k) = 0, \\ X_l \leq \mathbf{x}(k) \leq X_u, V_l \leq \boldsymbol{\nu}(k) \leq V_u, W_l \leq \boldsymbol{\omega}(k) \leq W_u. \end{cases} \end{aligned} \quad (47)$$

where the ranges of $\mathbf{x}(k)$, $\boldsymbol{\nu}(k)$ and $\boldsymbol{\omega}(k)$ are set as $15 \leq \|\mathbf{x}\|_\infty \leq 19$, $-0.3 \leq \|\boldsymbol{\nu}\|_\infty \leq 0.3$ and $-0.03 \leq \|\boldsymbol{\omega}\|_\infty \leq 0.03$, resp. The positive integer T is derived from the definition T -Detectability in [37]. It represents the number of steps a faulty model needs to generate an abnormal trajectory, such that the fault can be detected. We refer readers to [37] for more details about the computation method of T .

5.2.4. Results. In the simulation, we run the radiant system for 40 steps to generate data. In the first case, we assume $(A_{rad,2}^d, E_{rad,2}^d, C_{rad,2})$ occurs at $k = 20$. Figure 7 depicts the diagnosis results. Figure 7(a) shows the changes of the measured temperatures. The temperature T_1 decreases greatly due to the sensor failure, and other measured temperatures also change slightly because of the fault in pump 2. Figure 7(b) presents the changes of the residuals generated by the designed filters and feasibility of the invalidation problem (47). It can be seen that the residual r_1 is always below the threshold before $k = 20$. After the transition happens, r_1 crosses the threshold at $k = 21$ and the fault is detected. At $k = 23$, r_2 reaches the thresholds. It indicates that the first faulty mode is determined. Meanwhile, the problem (47) becomes infeasible at $k = 21$ after the transition happens, which means the transition is detected by the model invalidation method. In the second case, the faulty mode $(A_{rad,3}^d, E_{rad,3}^d, C_{rad,3})$ happens at $k = 20$. One can see from Figure 8(a) that the changes in the measured temperatures are slight. This poses a challenge to the diagnosis task. Figure 8(b) shows the changes of the residuals and feasibility of (47). It can be seen that r_1 crosses the threshold at $k = 22$. Hence, the fault is detected. Then r_3 reaches the threshold at $k = 24$, such that the second faulty mode is determined. As a comparison, the invalidation problem is always

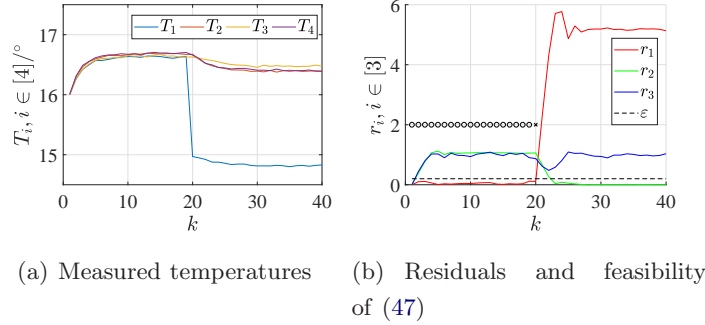


FIGURE 7. Simulation results with faulty mode 1 at $k = 20$, \circ meaning feasible and \times meaning infeasible

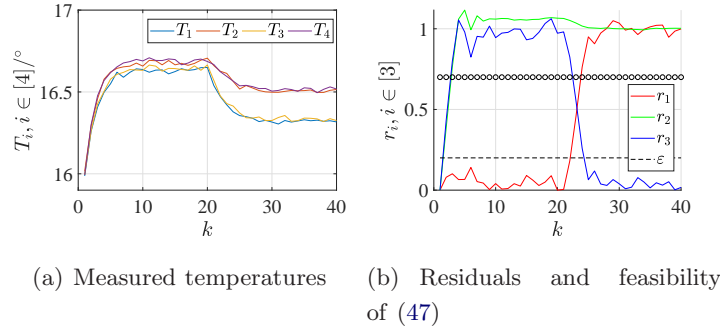


FIGURE 8. Simulation results with faulty mode 2 at $k = 20$

feasible during the diagnosis process, which means that the invalidation approach fails to detect the transition in the second case.

6. CONCLUSION AND FUTURE DIRECTIONS

In this paper, we developed a diagnosis scheme to detect the active mode of discrete-time, switched affine systems in the presence of stochastic measurement noise. Based on an integration of residual generation and \mathcal{H}_2 -norm approaches, the design of an optimal bank of filters is formulated into a tractable optimization problem in which the noise contribution to the residuals is minimized. With the designed filters, the diagnosis thresholds are determined which provide probabilistic false-alarm guarantees on the mode detection performance. Simulation results of a numerical example and a building radiant system show the effectiveness and performance of the proposed approach. As future work, the first research direction is combining the proposed approach with the active fault diagnosis method to deal with the unknown disturbance. One can design certain input sequences such that the unmatched residuals are separated from the matched residual with guaranteed probability. Note that the switching delay between the active mode and its corresponding controller is stochastic because of the stochastic noise. As a result, the second research direction would be focused on the impacts of the stochastic delay on the stability of asynchronously switched systems.

REFERENCES

- [1] V. Venkatasubramanian, R. Rengaswamy, K. Yin, S. N. Kavuri, A review of process fault detection and diagnosis: Part I: Quantitative model-based methods, *Computers & Chemical Engineering* 27 (3) (2003) 293–311.

- [2] A. Zolghadri, Advanced model-based FDIR techniques for aerospace systems: Today challenges and opportunities, *Progress in Aerospace Sciences* 53 (2012) 18–29.
- [3] J. Weimer, J. Araujo, M. Amoozadeh, S. A. Ahmadi, H. Sandberg, K. H. Johansson, Parameter-invariant actuator fault diagnostics in cyber-physical systems with application to building automation, in: *Control of Cyber-Physical Systems*, Springer, 2013, pp. 179–196.
- [4] L. Bako, Identification of switched linear systems via sparse optimization, *Automatica* 47 (4) (2011) 668–677.
- [5] H. Ohlsson, L. Ljung, Identification of switched linear regression models using sum-of-norms regularization, *Automatica* 49 (4) (2013) 1045–1050.
- [6] G. Ackerson, K. Fu, On state estimation in switching environments, *IEEE Transactions on Automatic Control* 15 (1) (1970) 10–17.
- [7] H. Lin, P. J. Antsaklis, Stability and stabilizability of switched linear systems: a survey of recent results, *IEEE Transactions on Automatic control* 54 (2) (2009) 308–322.
- [8] S. Yuan, L. Zhang, B. De Schutter, S. Baldi, A novel lyapunov function for a non-weighted L_2 gain of asynchronously switched linear systems, *Automatica* 87 (2018) 310–317.
- [9] Z. Gao, C. Cecati, S. X. Ding, A survey of fault diagnosis and fault-tolerant techniques—part I: Fault diagnosis with model-based and signal-based approaches, *IEEE Transactions on Industrial Electronics* 62 (6) (2015) 3757–3767.
- [10] R. V. Beard, Failure accomodation in linear systems through self-reorganization., Ph.D. thesis, Massachusetts Institute of Technology (1971).
- [11] D. Henry, A. Zolghadri, Design and analysis of robust residual generators for systems under feedback control, *Automatica* 41 (2) (2005) 251–264.
- [12] E. Chow, A. Willsky, Analytical redundancy and the design of robust failure detection systems, *IEEE Transactions on Automatic Control* 29 (7) (1984) 603–614.
- [13] E. Frisk, M. Nyberg, A minimal polynomial basis solution to residual generation for fault diagnosis in linear systems, *Automatica* 37 (9) (2001) 1417–1424.
- [14] M. Nyberg, E. Frisk, Residual generation for fault diagnosis of systems described by linear differential-algebraic equations, *IEEE Transactions on Automatic Control* 51 (12) (2006) 1995–2000.
- [15] R. Seliger, P. M. Frank, Fault-diagnosis by disturbance decoupled nonlinear observers, in: *the 30th IEEE Conference on Decision and Control*, 1991, pp. 2248–2253.
- [16] M. Benosman, A survey of some recent results on nonlinear fault tolerant control, *Mathematical Problems in Engineering* 2010 (2010).
- [17] F. Boem, R. M. Ferrari, T. Parisini, Distributed fault detection and isolation of continuous-time non-linear systems, *European Journal of Control* 17 (5-6) (2011) 603–620.
- [18] R. M. Ferrari, T. Parisini, M. M. Polycarpou, Distributed fault detection and isolation of large-scale discrete-time nonlinear systems: An adaptive approximation approach, *IEEE Transactions on Automatic Control* 57 (2) (2011) 275–290.
- [19] P. M. Esfahani, J. Lygeros, A tractable fault detection and isolation approach for nonlinear systems with probabilistic performance, *IEEE Transactions on Automatic Control* 61 (3) (2015) 633–647.
- [20] M. Halimi, G. Millérioux, J. Daafouz, Model-based modes detection and discernibility for switched affine discrete-time systems, *IEEE Transactions on Automatic Control* 60 (6) (2014) 1501–1514.
- [21] F. Küsters, S. Trenn, Switch observability for switched linear systems, *Automatica* 87 (2018) 121–127.
- [22] P. M. Frank, Fault diagnosis in dynamic systems using analytical and knowledge-based redundancy: A survey and some new results, *Automatica* 26 (3) (1990) 459–474.
- [23] V. Cocquempot, T. El Mezayani, M. Staroswiecki, Fault detection and isolation for hybrid systems using structured parity residuals, in: *the 5th Asian Control Conference*, Vol. 2, IEEE, 2004, pp. 1204–1212.
- [24] D. Wang, K. Y. Lum, Adaptive unknown input observer approach for aircraft actuator fault detection and isolation, *International Journal of Adaptive Control and Signal Processing* 21 (1) (2007) 31–48.
- [25] Z. Zhang, S. Li, H. Yan, Q. Fan, Sliding mode switching observer-based actuator fault detection and isolation for a class of uncertain systems, *Nonlinear Analysis: Hybrid Systems* 33 (2019) 322–335.

- [26] J. K. Scott, R. Findeisen, R. D. Braatz, D. M. Raimondo, Input design for guaranteed fault diagnosis using zonotopes, *Automatica* 50 (6) (2014) 1580–1589.
- [27] F. Harirchi, N. Ozay, Guaranteed model-based fault detection in cyber–physical systems: A model invalidation approach, *Automatica* 93 (2018) 476–488.
- [28] F. Boem, S. Rivero, G. Ferrari-Trecate, T. Parisini, Plug-and-play fault detection and isolation for large-scale nonlinear systems with stochastic uncertainties, *IEEE Transactions on Automatic Control* 64 (1) (2018) 4–19.
- [29] X. Chang, G. Yang, New results on output feedback H_∞ control for linear discrete-time systems, *IEEE Transactions on Automatic Control* 59 (5) (2013) 1355–1359.
- [30] J. Dong, A. S. Kolarijani, P. M. Esfahani, Multimode diagnosis for switched affine systems, in: 2021 American Control Conference (ACC), IEEE, 2021, pp. 870–875.
- [31] R. Vershynin, High-dimensional probability: An introduction with applications in data science, Vol. 47, Cambridge university press, 2018.
- [32] P. Rosa, C. Silvestre, On the distinguishability of discrete linear time-invariant dynamic systems, in: 2011 50th IEEE Conference on Decision and Control and European Control Conference, IEEE, 2011, pp. 3356–3361.
- [33] M. C. De Oliveira, J. C. Geromel, J. Bernussou, Extended H_2 and H_∞ norm characterizations and controller parametrizations for discrete-time systems, *International Journal of Control* 75 (9) (2002) 666–679.
- [34] C. D. Meyer, Matrix analysis and applied linear algebra, Vol. 71, Siam, 2000.
- [35] C. V. D. Ploeg, M. Alirezaei, N. V. D. Wouw, P. M. Esfahani, Multiple faults estimation in dynamical systems: Tractable design and performance bounds (2020). [arXiv:2011.13730](https://arxiv.org/abs/2011.13730).
- [36] J. Lfberg, Yalmip : A toolbox for modeling and optimization in matlab, in: Proceedings of the CACSD Conference, 2004.
- [37] F. Harirchi, N. Ozay, Guaranteed model-based fault detection in cyber–physical systems: A model invalidation approach, *Automatica* 93 (2018) 476–488.